Macromolecules **1999,** *32,* 6963−6968

Synthesis of Poly(α-methylstyrene-*b*-isobutylene) Copolymers by Living Cationic Sequential Block Copolymerization: Investigation on the Crossover from Living Poly(α-methylstyrene) Chain End to Isobutylene

Younghwan Kwon, Xianyi Cao, and Rudolf Faust*

Polymer Science Program, Department of Chemistry, University of Massachusetts Lowell,
One University Avenue, Lowell, Massachusetts 01854

Received March 4, 1999; Revised Manuscript Received August 16, 1999

ABSTRACT: The synthesis of poly(α-methylstyrene-*b*-isobutylene) (P(αMeSt-*b*-IB)) copolymers via sequential monomer addition was studied using the adduct of the olefinic αMeSt dimer and HCl (DiαMeSt·HCl) as initiator in the presence of 2,6-di-*tert*-butylpyridine (DTBP) in methylcyclohexane (MeChx)/methyl chloride (MeCl) (60/40 v/v) at −80 °C. With BCl_3 employed as co-initiator in the first step of the synthesis, well-defined PαMeSt with controlled molecular weight and narrow molecular weight distribution ($\bar{M}_w/\bar{M}_n = 1.05 \sim 1.20$) was obtained. Chain end decomposition was not detected for up to 30 min under monomer-starved condition. Model reactions using DiαMeSt·HCl indicated that, upon addition of IB, quantitative crossover takes place followed by immediate termination and the selective formation of PαMeSt-IB_1-Cl. Therefore, the addition of $TiCl_4$ was necessary to polymerize IB. The obtained P(αMeSt-*b*-IB) diblock copolymer was found to be contaminated by a small amount of homo P(αMeSt), apparently formed via intramolecular alkylation. It has been shown that the blocking efficiency (B_{eff}) was a linear function of [IB], but this appeared to be very different for DiαMeSt-IB_1-Cl and PαMeSt-IB_1-Cl. This difference was attributed to selective solvation of PαMeSt-IB_1-Cl by the solvent, which results in local [IB], which is about one-tenth of that in the bulk.

Introduction

Block copolymers have been and continue to be the subject of scientific and practical interest because of their remarkable architecture/property relationships, which arise mainly when thermodynamically incompatible polymer blocks are combined.[1−6] Since the concept of the living cationic polymerization was introduced in the eighties,[7,8] the cationic synthesis of block copolymers has been extensively studied. Living cationic sequential block copolymerization is generally recognized as one of the most powerful and straightforward methods to obtain well-controlled block copolymers with high structural integrity.[9] However, the clean synthesis of block copolymers by sequential monomer addition requires that the rate of a crossover reaction to a second monomer be faster than or at least equal to that of homopolymerization of a second monomer. This can be controlled by the judicious selection of polymerization conditions; mainly by selecting the appropriate order of monomer addition.

In the course of our studies in living cationic sequential block copolymerization, the intermediate capping of the living PIB with nonhomopolymerizable monomers such as 1,1-diphenylethylene (DPE) and its derivatives was invented to achieve sequential block copolymerization of IB with more reactive monomers. Upon tuning the Lewis acidity to the reactivity of the second monomer, the diphenylcarbenium ion, which arises after capping of living PIB with DPE, was found to efficiently initiate the living polymerization of reactive monomers such as *p*-methylstyrene (pMeSt),[10,11] αMeSt,[12,13] isobutyl vinyl ether,[14] and methyl vinyl ether.[15] This methodology has also been successfully applied to the synthesis of poly(pMeSt-*b*-IB-*b*-pMeSt) and poly(αMeSt-*b*-IB-*b*-αMeSt) thermoplastic elastomers (TPEs).

While the recent discovery of coupling reactions of living cationic polymers allows one to synthesize TPEs via sequential monomer addition, followed by coupling[16,17] using the reverse order of monomer addition, no report has yet been published on the living cationic sequential block copolymerization from a more reactive monomer to IB.

The aim of the present study is to investigate the synthesis of P(αMeSt-*b*-IB) copolymers via living cationic sequential polymerization of αMeSt and IB. Several reports on the living cationic polymerization of αMeSt have already been published.[18−22] We recently reported the living cationic polymerization of αMeSt initiated by DiαMeSt·HCl/BCl_3, in the presence of DTBP as a proton trap, using MeChx/MeCl (60/40 v/v) solvent mixture at −80 °C.[23] However, the weak Lewis acids used in these studies are unsuitable for the polymerization of IB. Therefore, the present investigation is focused on selecting the most suitable initiating system for the living cationic polymerization of αMeSt and identifying optimum conditions for block copolymerization with IB via sequential monomer addition utilizing $TiCl_4$ as the Lewis acid (which is necessary to obtain high molecular weight PIB) in a one-pot procedure. Furthermore, mechanistic studies on the early crossover step and propagation using model reaction will be discussed.

Experimental Section

Materials. 2-Chloro-2,4-diphenyl-4-methylpentane (DiαMeSt·HCl) and 2-chloro-2,4,6-triphenyl-4,6-dimethylheptane (TriαMeSt·HCl) were prepared by hydrochlorination of 2,4-diphenyl-4-methyl-1-pentene (DiαMeSt-ene, Aldrich) and 2,4,6-triphenyl-4,6-dimethyl-1-heptene (TriαMeSt-ene), respectively.[22] All other chemicals and solvents were purified as described previously[12,13,20] or used as received.

Synthesis of TriαMeSt-ene. TriαMeSt-ene was prepared in a 150 mL test tube under nitrogen atmosphere at −80 °C. MeChx, trimethyl(2-phenyl-2-propenyl)silane (7.4×10^{-2} M), DTBP (3.0×10^{-3} M), DiαMeSt·HCl (3.7×10^{-2} M) stock

10.1021/ma990333k CCC: $18.00

solution, and MeCl were added sequentially to a prechilled 150 mL test tube. BCl_3 (0.11 M), dissolved in MeChx, was added last. After 30 min, the reaction was terminated with prechilled methanol. Purification by dissolution/precipitation in hexane/methanol followed by column chromatography on silica gel (200−400 mesh, 60 Å, Aldrich) eluting with hexane gave the pure compound (0.75 g, 95.1% yield) as a colorless liquid: 250 MHz ^{1}H NMR ($CDCl_3$) δ 7.26−7.15 (15H, Ar), 5.05 (1H, $CH_2=$), 4.68 (1H, $CH_2=$), 2.75 (2H, $-CH_2-$), 2.30 (2H, $-CH_2-$), 1.12 (3H, CH_3), 0.87 (3H, CH_3), 0.74 (3H, CH_3); 60 MHz ^{13}C NMR ($CDCl_3$) δ 151.0, 148.4, 146.7, 144.5, 128.3, 128.2, 127.9, 127.2, 127.0, 127.0, 126.3, 125.6, 125.5, 118.0, 56.1, 52.5, 43.2, 38.7, 35.1, 28.1, 23.9.

Synthesis of Trimethyl(2-phenyl-2-propenyl)silane.[24] To a mixture of αMeSt (10 mL, 77 mmol) and *t*-BuOK (9.0 g, 80 mmol) in THF (200 mL) at −78 °C was added *n*-BuLi (32 mL, 80 mmol, 2.5 M in hexane) dropwise over a period of 30 min. The mixture was stirred at −78 °C for 5 h. The reaction mixture was transferred at −78 °C to another 500 mL three-neck round-bottomed flask containing a solution of chlorotrimethylsilane (10.1 mL, 93 mmol) in THF (100 mL). The mixture was stirred for an additional 30 min and then allowed to warm up to room temperature. Subsequently the dark red suspension was poured into 500 mL of distilled water and the product was extracted with hexane (200 mL × 2). The combined organic layer was dried over $MgSO_4$. Removal of solvent under reduced pressure followed by vacuum distillation gave the pure compound (2.93 g, 20.0% yield) as a colorless liquid: 250 MHz ^{1}H NMR ($CDCl_3$) δ 7.51−7.33 (5H, Ar), 5.20 (1H, $CH_2=$), 4.95 (1H, $CH_2=$), 2.11 (2H, $-CH_2-$), 0.00 (9H, $(CH_3)_3$).

Polymerization. Polymerizations were carried out in a 75 mL test tube at −80 °C under a dry ($[H_2O] < 1.0$ ppm) nitrogen atmosphere in an MBraun 150-M glovebox (Innovative Technology Inc.). A representative polymerization procedure of αMeSt was as follows: MeChx, αMeSt (0.35 M), DTBP as a proton trap (3×10^{-3}M), DiαMeSt·HCl initiator stock solution (2×10^{-3}M), and MeCl were added sequentially to a prechilled 75 mL test tube. Then BCl_3, dissolved in MeChx, was added last. At predetermined time intervals, the polymerizations were terminated by adding prechilled methanol. The polymers were purified by dissolution-precipitation in CH_2Cl_2/methanol and dried in a vacuum prior to GPC measurement. To study the lifetime of PαMeSt chain ends the incremental monomer addition (IMA) technique was employed; after complete conversion of the first αMeSt increment a second αMeSt increment was added to the polymerization mixture at a different time and polymerized.

The living cationic sequential block copolymerization of αMeSt and IB was carried out by introducing IB to the test tube after complete polymerization of αMeSt, followed by addition of $TiCl_4$ (3.64×10^{-2} M) stock solution.

Characterization. Molecular weights and molecular weight distributions were measured using two GPC (Gel Permeation Chromatography) systems. One was equipped with a model 510 pump, a model 410 differential refractometer, a model 441 UV/vis detector, on line multiangle laser light scattering detector (MALLS, MiniDawn, Wyatt Technology, Inc.), a model 712 sample processor, and five Ultrastyragel GPC columns connected in the following series: 500, 10^3, 10^4, 10^5, and 100 Å. The other system was equipped with a model 510 pump, a model 486 tunable UV/vis detector, a model 250 dual refractometer/viscometer detector (Viscotek), a model 712 sample processor, and five Ultrastyragel columns connected in the same series as for the MALLS system. The flow rate of THF, which was used as an eluent on both systems, was 1.0 mL/min. For data analysis, the UV detector signals were simultaneously recorded on a PC and used for calculating the B_{eff} of the block copolymers with peak analysis software (PeakFit v3.10, Jandel Scientific). ^{1}H NMR and ^{13}C NMR spectra were recorded on Bruker spectrometers (250 and 500 MHz) using $CDCl_3$ as a solvent (Cambridge Isotope Laboratories, Inc.).

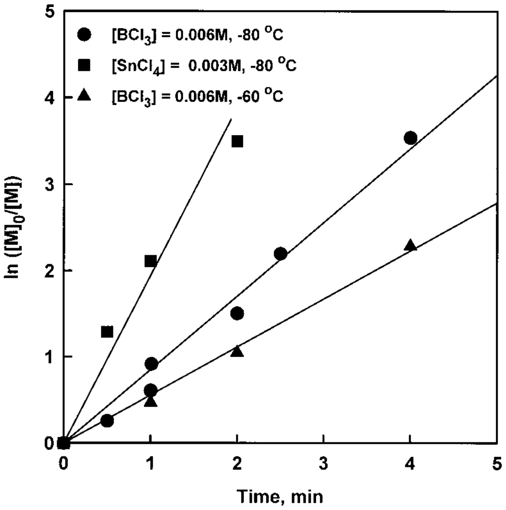

Figure 1. Effect of Lewis acids and temperature on the rate of polymerization of αMeSt. Other polymerization conditions: [αMeSt] = 0.35 M, [DiαMeSt·HCl] = 0.002 M, [DTBP] = 0.003 M, and MeChx/MeCl = 60/40 (v/v).

Results and Discussion

Living Cationic Polymerization of αMeSt. First, we investigated the effect of Lewis acid and temperature on the polymerization of αMeSt using DiαMeSt·HCl as an initiator, in the presence of DTBP as a proton trap, in MeChx/MeCl (60/40 v/v) solvent mixture. As Lewis acids, only metal chlorides, $SnCl_4$ and BCl_3, were employed to avoid ligand exchange upon addition of $TiCl_4$, resulting in titanium compounds of lower Lewis acidity that are unsuitable for the polymerization of IB.

At −80 °C, a linear first-order kinetic plot (Figure 1) was obtained with BCl_3, indicating a constant number of active chains, i.e., the absence of irreversible termination during the entire polymerization period. The plot with $SnCl_4$ (Figure 1) however, deviates somewhat from linearity, which may indicate termination (sampling at <1 min is difficult and may not be accurate due to the high rate of the polymerization). Rapid termination under monomer starved condition was indeed confirmed by IMA experiments (see later). The k_{app}s ($=k_p$ [P$^+$]) obtained were 1.4×10^{-2} s^{-1} and $\sim 3 \times 10^{-2}$ s^{-1} for BCl_3 and $SnCl_4$ co-initiators, respectively. The $\bar{M}_n$ and $\bar{M}_w/\bar{M}_n$ vs conversion plots are shown in Figure 2. The linear $\bar{M}_n$ vs conversion plots for both Lewis acids demonstrated the absence of chain transfer during the polymerization. Importantly, the polymers exhibited close to theoretical $\bar{M}_n$s indicating ~100% initiator efficiency (I_{eff}) and narrow molecular weight distributions decreasing with increasing conversions ($\bar{M}_w/\bar{M}_n = 1.05-1.20$ at close to complete monomer conversion).

The effect of temperature on the living cationic polymerization of αMeSt was studied using DiαMeSt·HCl/BCl_3/DTBP in MeChx/MeCl (60/40 v/v) at −80 °C and −60 °C. The ln([M]$_0$/[M]) vs time plot at −60 °C (Figure 1) was also linear, indicating the absence of irreversible termination. In comparison to $k_{app} = 1.4 \times 10^{-2}$ s^{-1} at −80 °C, k_{app} was calculated to be 0.9×10^{-2} s^{-1} at −60 °C. The increase in k_{app} with decreasing temperature may be explained by the negative apparent activation energy, a result of the higher extent of chain end ionization at lower temperature.[25,26] Recently we also reported negative apparent activation energy (−3.5 kcal/mol) for the living cationic polymerization of αMeSt.[22] The $\bar{M}_n$s and $\bar{M}_w/\bar{M}_n$s at −60 °C are plotted

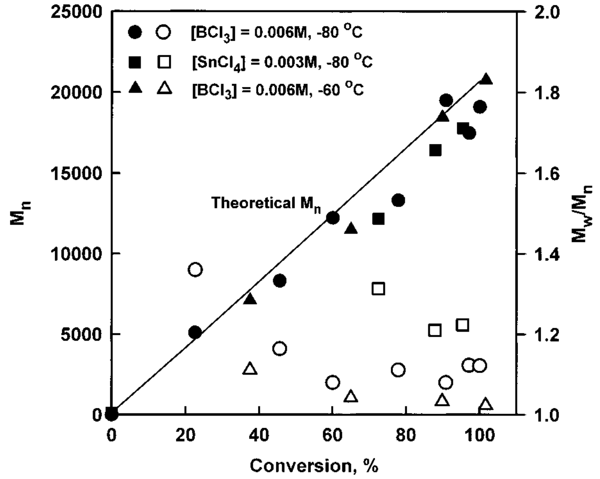

Figure 2. $\bar{M}_n$ and $\bar{M}_w/\bar{M}_n$ vs conversion plots for the polymerization of αMeSt. Other polymerization conditions: same as in Figure 1. Key: filled symbols, $\bar{M}_n$; open symbols, $\bar{M}_w/\bar{M}_n$.

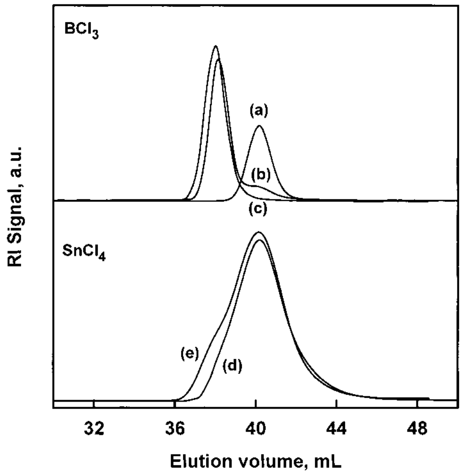

Figure 3. GPC traces of PαMeSt by incremental monomer addition (IMA) technique: (a) original PαMeSt at −80 °C; (b) PαMeSt after 8 min monomer-starved condition at −60 °C; (c) PαMeSt after 30 min at −80 °C; (d) original PαMeSt at −80 °C; (e) PαMeSt after 2 min at −80 °C. Other polymerization conditions: same as Figure 1.

against conversion in Figure 2. The $\bar{M}_n$s were close to the theoretical values, and narrow $\bar{M}_w/\bar{M}_n$s were also obtained at −60 °C.

To examine the lifetime of the PαMeSt living end, after complete conversion of the first αMeSt increment a second αMeSt increment was added to the polymerization mixture at different time and was polymerized for an additional 5 min. The GPC traces of the products obtained at −80 and −60 °C are compared in Figure 3. Using BCl_3 at −80 °C, a second αMeSt increment was added to the polymerization mixture after 30 min of monomer starved condition. The $\bar{M}_n$ s approximately doubled, and $\bar{M}_w/\bar{M}_n$ values remained narrow after the complete consumption of the second monomer increment, demonstrating that decomposition of living PαMeSt chain end in 30 min under this condition was undetectable. At −60 °C, however, the living PαMeSt chain ends decomposed rapidly. The GPC traces indicated that ca. 29% of the PαMeSt chain end underwent irreversible termination in 8 min under monomer-starved conditions at −60 °C (Figure 3b). With $SnCl_4$ at −80 °C, almost complete decomposition of PαMeSt chain end was observed within 2 min under monomer-starved conditions (Figure 3e).

Scheme 1

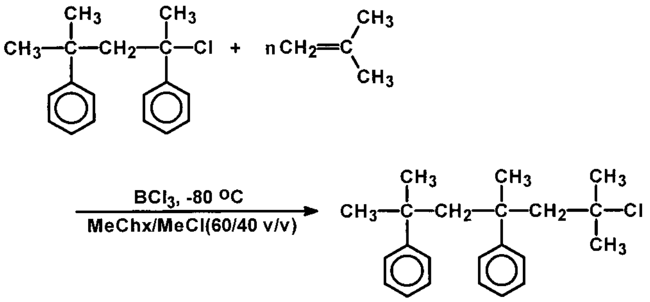

Thus, considering our ultimate goal as the synthesis of the P(αMeSt-*b*-IB) copolymer via sequential monomer addition, the DiαMeSt·HCl/BCl_3/DTBP system in MeChx/MeCl (60/40 v/v) solvent mixture at −80 °C is preferred for the living cationic polymerization of αMeSt.

Polymerization of IB Using DiαMeSt·HCl Initiator as a Model Reaction for the Synthesis of P(αMeSt-*b*-IB) Copolymer. The crossover from living PαMeSt chain end to IB was studied using DiαMeSt·HCl as a model compound that mimics the PαMeSt chain end. DiαMeSt·HCl was reacted with BCl_3 for 40 min in MeChx/MeCl (60/40 v/v) solvent mixture at −80 °C, and then IB was added (Scheme 1). It was found that fast and quantitative crossover to IB was followed by instantaneous termination and thus the selective formation of the DiαMeSt-IB_1-Cl (1:1 adduct of DiαMeSt·HCl and IB) was observed: 250 MHz ^{1}H NMR ($CDCl_3$) δ 7.00−7.20 (10H, Ar), 2.34, 2.28, 2.12, and 2.08 (*dd*, 2H, $-CH_2-$), 2.14 (2H, $-CH_2-$), 1.14 (3H, CH_3), 1.09 (3H, CH_3), 1.06 (3H, (CH_3)CCl), 1.05 (3H, (CH_3)CCl), 0.80 (3H, CH_3); 60 MHz ^{13}C NMR ($CDCl_3$) δ 150.6, 148.0, 128.3, 128.3, 127.6, 126.3, 126.0, 125.7, 72.3, 60.3, 59.5, 43.4, 39.0, 36.4, 34.8, 33.4, 28.4, 23.9. Similarly, the polymerization of IB did not take place using cumyl chloride in conjunction with BCl_3 in MeChx/MeCl (60/40 v/v) solvent at −80 °C, and the 1:1 adduct of cumyl chloride and IB was quantitatively formed. These results are in accord with known solvent dependent co-initiating activity of BCl_3, i.e., ionization of the $-CH_2-C(CH_3)_2-Cl$ chain end only occurs in polar solvents. On the basis of these results, it was concluded that the crossover from DiαMeSt·HCl to IB is quantitative, giving rise to the selective formation of DiαMeSt-IB_1-Cl. Therefore, a stronger Lewis acid such a $TiCl_4$ is necessary for further propagation of IB under these conditions.

To find optimum reaction conditions for the polymerization of IB from living PαMeSt chain end, we extended our studies to the living cationic polymerization of IB using the DiαMeSt·HCl/BCl_3 and/or $TiCl_4$/DTBP system in MeChx/MeCl (60/40 v/v) at −80 °C. The effect of addition order of reagents such as IB and Lewis acids on the living cationic polymerization was examined. The first series of IB polymerization was carried out by adding $TiCl_4$ to the solution of DiαMeSt·HCl and IB. In the second series of experiments, which closely resembles the conditions of sequential block copolymerization, BCl_3 was added to the solution containing DiαMeSt·HCl, followed by IB and finally $TiCl_4$. The third series of experiments was performed by the addition of BCl_3 and $TiCl_4$ to the solution of DiαMeSt·HCl, immediately followed by the addition of IB. The results are shown in Figure 4 and Figure 5.

In the first and second series of experiments, ~100% IB conversion was reached in 60 min, and the linear

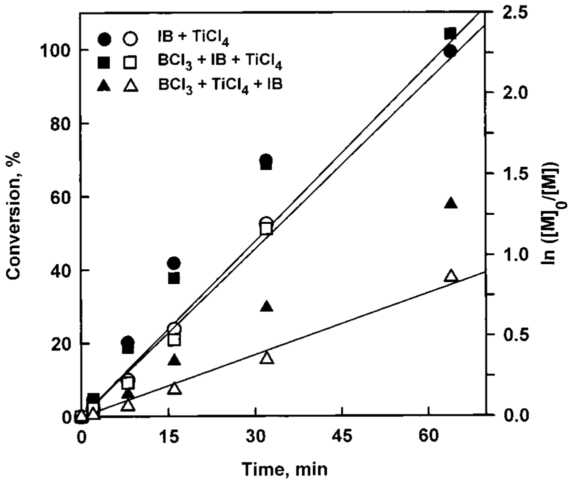

Figure 4. Conversion and $\ln([M]_0/[M])$ vs time plots in the polymerization of IB at −80 °C. Polymerization conditions: [IB] = 1.426 M, [DiαMeSt·HCl] = 0.002 M, $[BCl_3]$ = 0.006 M, $[TiCl_4]$ = 0.036 M, and MeChx/MeCl = 60/40 v/v. Key: filled symbols, conversion; open symbols, $\ln([M]_0/[M])$.

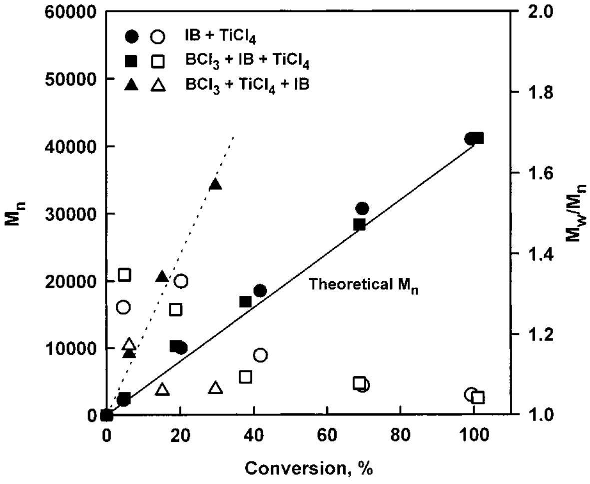

Figure 5. $\bar{M}_n$ and $\bar{M}_w/\bar{M}_n$ vs conversion plots in the polymerization of IB at −80 °C. Polymerization conditions: same as Figure 4. Key: filled symbols, $\bar{M}_n$; open symbols, $\bar{M}_w/\bar{M}_n$.

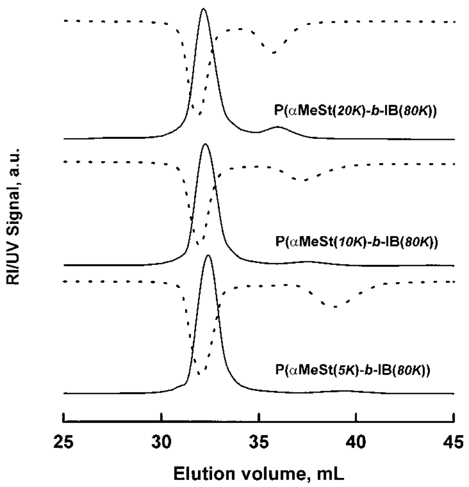

Figure 6. GPC traces of P(αMeSt-*b*-IB) copolymer with different molecular weight of PαMeSt obtained via living cationic sequential block copolymerization of αMeSt and IB. Key: (—) RI detection; (- - -) UV detection at 254 nm.

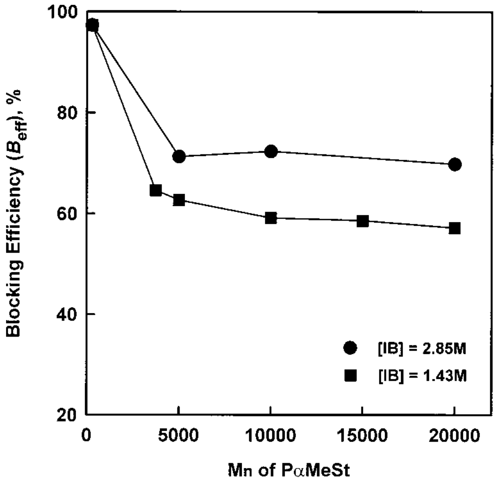

Figure 7. Effect of chain lengths of PαMeSt and concentrations of IB on the blocking efficiency (B_{eff}) for the synthesis of PαMeSt-*b*-IB copolymers.

first-order kinetic plots (Figure 4) and linear $\bar{M}_n$ vs conversion plots (Figure 5) indicated the absence of termination and chain transfer to monomer. In the third series of IB polymerization, a linear first-order kinetic plot (Figure 4) was also obtained, demonstrating the absence of irreversible termination. However, the polymerization was almost three times slower than that of the other two systems, yielding only ~60% conversion in 1 h. The $\bar{M}_n$ s vs conversion plot was linear (Figure 5), but it was well above the theoretical line, indicating low I_{eff}. This low I_{eff} strongly suggested a side reaction, most likely by intramolecular back biting (indanyl ring formation), upon ionization of DiαMeSt·HCl with $TiCl_4$ in the absence of IB.[27] On the basis of these results, it was concluded that $TiCl_4$ is necessary for the polymerization of IB; however, $TiCl_4$ should be added last to avoid side reactions in the synthesis of P(αMeSt-*b*-IB) copolymers via sequential monomer addition.

Synthesis of P(αMeSt-*b*-IB) Copolymers by Sequential Monomer Addition. For the synthesis of P(αMeSt-*b*-IB) copolymers, living PαMeSt with different chain lengths was first obtained using the DiαMeSt·HCl/BCl_3/DTBP/MeChx:MeCl(60:40 v:v)/−80 °C system, followed by the addition of IB. From the resulting PαMeSt-IB_1-Cl chain end, IB was further polymerized by the addition of $TiCl_4$. Figure 6 shows typical GPC traces of the P(αMeSt-*b*-IB) copolymers measured using both refractive-index (RI) and ultraviolet (UV at $\lambda = 254$ nm) detectors. As shown in Figure 6, the GPC RI traces of P(αMeSt-*b*-IB) copolymers shifted toward higher molecular weight. However, a small peak at a position, identical to that of the PαMeSt homopolymer, was found in both RI and UV traces, indicating that a small amount of PαMeSt homopolymer remained even after complete conversion of IB. The area of UV traces was used to calculate the B_{eff} (100 × weight of PαMeSt in P(αMeSt-*b*-IB) block copolymer/total weight of PαMeSt, %) by PeakFit software using exponential Gaussian distribution.

From Figure 6, the B_{eff} was calculated and plotted as a function of $\bar{M}_n$ for PαMeSt block segment in Figure 7. At 1.43 and 2.85 M of IB concentrations, the B_{eff}s were calculated to be approximately 60% and 70%, respectively, regardless of the chain lengths of living PαMeSt in the $\bar{M}_n$ = 3000−20 000 range. This was surprising in view of the efficient crossover observed with DiαMeSt-IB_1-Cl. The previous study of the model reaction of DiαMeSt·HCl and IB in the presence of BCl_3 has demonstrated the quantitative formation of DiαMeSt-

Scheme 2

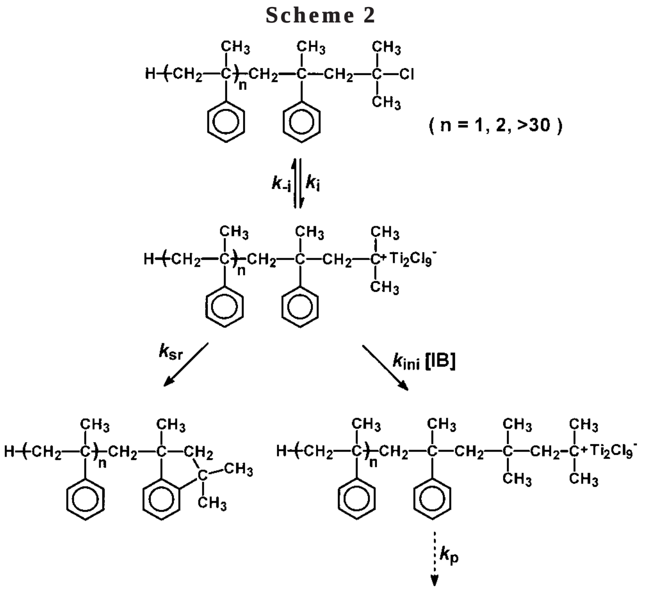

IB_1-Cl. Since BCl_3 is unable to ionize DiαMeSt-IB_1-Cl, we postulated that the lower than 100% B_{eff} is due to side reactions after the addition of $TiCl_4$. To identify the side reaction, DiαMeSt-IB_1-Cl was aged with $TiCl_4$ in the absence of IB for 40 min. ^1H and ^{13}C NMR spectroscopy confirmed that the major product of this side reaction was the indanyl ring compound of DiαMeSt-IB_1-Cl via intramolecular alkylation: 250 MHz ^1H NMR ($CDCl_3$) δ 7.43−7.04 (9H, Ar), 2.47, 2.42, 1.98, and 1.92 (*dd*, 2H, $-CH_2-$ (indanyl ring)), 2.03, 1.98, 1.62, and 1.55 (*dd*, 2H, $-CH_2-$), 1.39 (3H, CH_3), 1.33 (3H, CH_3 (indanyl ring)), 1.21 (3H, CH_3 (indanyl ring)), 1.18 (3H, CH_3), 0.95 (3H, CH_3); 60 MHz ^{13}C NMR ($CDCl_3$) δ 153.0, 150.9, 150.8, 128.4, 127.1, 126.9, 126.4, 125.7, 123.3, 122.9, 56.6, 54.8, 47.6, 43.2, 39.1, 34.3, 32.4, 31.7, 31.3, 29.2. After fractionation of the block copolymer from dead P(αMeSt), the terminal structure of the dead P(αMeSt) was also investigated using 500 MHz ^1H NMR spectroscopy. The same characteristic $-CH_2-$ (indanyl ring) peaks (at approximately 2.5 ppm) were conspicuously observed, indicating that termination is due to indanyl ring formation.

Considering that indanyl ring formation is zero-order in IB concentration ($R_{sr} = k_{sr}[P+]$) and initiation of IB is first-order in IB concentration ($R_{ini} = k_{ini}[P+][IB]$) (Scheme 2), the relative rate between initiation and side reaction can be expressed as follows:

$$\frac{R_{ini}}{R_{sr}} = \frac{I_{eff}}{1 - I_{eff}} = \frac{k_{ini}[P+]}{k_{sr}[P+]}[IB] \qquad (1)$$

R_{ini} and R_{sr} denote the rates of initiation and side reactions, and k_{ini} and k_{sr} also denote the rate constants of initiation and side reactions, respectively. [P+] and [IB] refer the concentrations of active species and IB, respectively. I_{eff} is defined as $R_{ini}/(R_{ini} + R_{sr})$. Assuming that R_{sr} remains constant with increasing chain length, it can be concluded from eq 1 that the relative ratio (R_{ini}/R_{sr}), which affects B_{eff} in the synthesis of P(αMeSt-*b*-IB) copolymer, depends solely on the concentration of IB.

To verify constant reactivity (R_{sr}) of the chain end, DiαMeSt-IB_1-Cl and TriαMeSt-IB_1-Cl were prepared in situ by reacting DiαMeSt·HCl and TriαMeSt·HCl, respectively, with an equimolar amount of IB in the presence of BCl_3 in MeChx/MeCl (60/40 v/v) at −80 °C and then aged with $TiCl_4$ for different times. IB was added after different aging times and polymerized for 120 min. The rate of decomposition of DiαMeSt-IB_1-Cl and TriαMeSt-IB_1-Cl with $TiCl_4$ was so fast that 77% and 85% of the chain end of the dimeric and the trimeric initiators were decomposed within 1 min aging time. Since the contribution of direct initiation of IB was observed under this condition (conversion = 9.43%, $\bar{M}_n$ = 108,500, $\bar{M}_w/\bar{M}_n$ = 1.41), the rate constants of decomposition of DiαMeSt-IB_1-Cl ($k_d = 2.38 \times 10^{-2}\ s^{-1}$) and TriαMeSt-$IB_1$-Cl ($k_d = 3.16 \times 10^{-2}\ s^{-1}$) were calculated from the results within the first minute. Even though the experimental error is large within 1 min aging time, the rate constant of decomposition, i.e., indanyl ring formation, can be considered to be independent of the chain length.

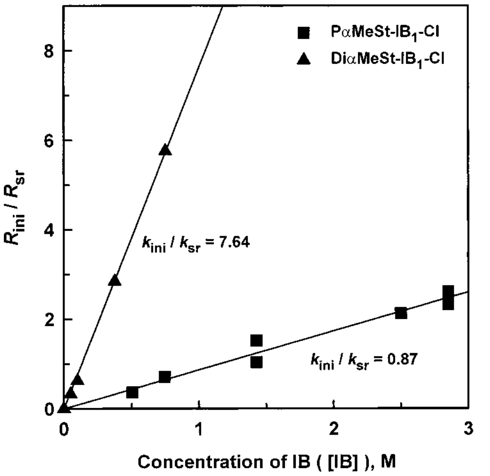

Figure 8. Dependence of IB concentrations on R_{ini}/R_{sr} values using DiαMeSt-IB_1-Cl (▲) and PαMeSt-IB_1-Cl (■, $\bar{M}_n$ = 20 000).

The effect of the concentration of IB on the R_{ini}/R_{sr} ratio was investigated using DiαMeSt-IB_1-Cl and PαMeSt-IB_1-Cl ($\bar{M}_n$ = 20 000). Figure 8 confirms that the R_{ini}/R_{sr} ratio is linearly dependent on the concentration of IB for both DiαMeSt-IB_1-Cl and PαMeSt-IB_1-Cl. However, from the slopes, k_{ini}/k_{sr}s for DiαMeSt-IB_1-Cl and PαMeSt-IB_1-Cl were calculated to be 7.46 and 0.87, respectively, indicating a much lower rate of initiation for PαMeSt-IB_1-Cl. According to eq 1, this can only be attributed to different local concentrations of IB around DiαMeSt-IB_1-Cl and PαMeSt-IB_1-Cl. On the basis of the k_{ini}/k_{sr} ratios for PαMeSt-IB_1-Cl and DiαMeSt-IB_1-Cl, the local concentration of IB around PαMeSt-IB_1-Cl is only about one-tenth (0.114) of that around DiαMeSt-IB_1-Cl, which can be assumed to be equal to that in the bulk. This difference appears to be the result of specific solvation of PαMeSt-IB_1-Cl by the solvent since IB is a poor solvent for PαMeSt.

Conclusion

The synthesis of P(αMeSt-*b*-IB) block copolymer via sequential monomer addition was studied. On the basis of mechanistic studies on the crossover and early propagation steps using model compounds, optimal conditions for the living cationic polymerization of αMeSt and IB have been identified. Well-controlled PαMeSt and PIB block segments have been achieved using DiαMeSt·HCl as initiator in combination with a suitable co-initiator, i.e., BCl_3 for αMeSt and $TiCl_4$ for IB, in the presence of DTBP in MeChx/MeCl(60/40 v/v) at −80 °C. It was shown that upon addition of IB to living PαMeSt in the presence of BCl_3 quantitative crossover takes place followed by instantaneous termination (initiation without propagation) and the selective formation of PαMeSt-IB_1-Cl. Propagation of IB was affected by adding $TiCl_4$. It was found that the B_{eff} (100 × weight of PαMeSt in P(αMeSt-*b*-IB) block copolymer/total weight of PαMeSt, %) was linearly dependent on the concentration of IB, but this effect was substantially different for dimeric and polymeric PαMeSt chain, which might be attributed to different local concentrations of IB. From the different rates of initiation with DiαMeSt-IB_1-Cl and PαMeSt-IB_1-Cl ($\bar{M}_n = 20\,000$) the local concentration of IB around PαMeSt-IB_1-Cl chain end was calculated to be about one-tenth of that around DiαMeSt-IB_1-Cl, which is assumed to be identical to [IB] in the bulk.

Acknowledgment. Financial support from the National Science Foundation (DMR-9806418 and DMR-9502777) and Exxon Chemical Co. is gratefully acknowledged. We also thank Dr. Zs. Fodor and Dr. B. Koroskenyi for their help in some experiments and NMR study.

Supporting Information Available: Figures showing ^1H and ^{13}C NMR spectra of DiαMeSt-IB_1-Cl and the indanyl ring product from DiαMeSt-IB_1-Cl and the ^1H NMR spectrum of the 1:1 adduct of cumyl chloride and IB. This material is available free of charge via the Internet at http://pubs.acs.org.

References and Notes

(1) Folkes, M. J., Ed. *Processing, Structure and Properties of Block Copolymers*; Elsevier: London, 1985.
(2) Meier, D. J., Ed. *Block Copolymers: Science and Technology*;, Harvard: New York, 1983.
(3) Salamone, J. C., Ed. *Polymeric Materials Encyclopedia*; CRC Press, Inc.: Boca Raton, FL, 1996; Vol. 1, pp 743−825.
(4) Lescanec, R. L.; Fetters, L. J.; Thomas, E. L. *Macromolecules* **1998**, *31*, 1680.
(5) Brinkmann, S.; Stadler, R.; Thomas, E. L. *Macromolecules* **1998**, *31*, 6566.
(6) Elbs, H.; Fukunaga, K.; Stadler, R.; Sauer, G.; Magerle, R.; Krausch, G. *Macromolecules* **1999**, *32*, 1204.
(7) Miayamoto, M.; Sawamoto, M.; Higashimura, T. *Macromolecules* **1984**, *17*, 265.
(8) Faust, R.; Kennedy, J. P. *Polym. Bull.* **1986**, *15*, 317; *J. Polym. Sci., Polym. Chem. Ed.* **1987**, *A25*, 1847.
(9) Sawamoto, M. *In Cationic Polymerization. Mechanism, Synthesis, and Application*, Matyjaszewski, K., Ed.; Marcel Dekker: New York, 1996; Chapter 5.
(10) Fodor, Zs.; Faust, R. *J. Macromol. Sci. Pure Appl. Chem.*. **1994**, *A31*, 1983.
(11) Fodor, Zs.; Faust, R. *J. Macromol. Sci. Pure Appl. Chem.*. **1995**, *A32*, 575.
(12) Li, D.; Faust, R. *Macromolecules* **1995**, *28*, 1383.
(13) Li, D.; Faust, R. *Macromolecules* **1995**, *28*, 4893.
(14) Hadjikriacou, S.; Faust, R. *Macromolecules* **1995**, *28*, 7893.
(15) Hadjikyriacou, S.; Faust, R. *Macromolecules* **1996**, *29*, 5261.
(16) Bae, Y. C.; Fodor, Zs.; Faust, R. *Macromolecules* **1997**, *30*, 198.
(17) Bae, Y. C.; Faust, R. *Macromolecules* **1998**, *31*, 2480.
(18) Higashimura, T.; Kamigaito, M.; Kato, M.; Hasebe, T.; Sawamoto, M. *Macromolecules* **1993**, *26*, 2670.
(19) Matyjaszewski, K.; Bon, A.; Lin, Ch.-H.; Xiang, J. S. *Polym. Prepr.* **1993**, *34* (1), 487.
(20) Li, D.; Hadjikyriacou, S.; Faust, R. *Macromolecules* **1996**, *29*, 6061.
(21) Li, D.; Hadjikyriacou, S.; Faust, R. *Polym. Prepr.* **1996**, *37* (1), 803.
(22) Fodor, Zs.; Faust, R. *J. Macromol. Sci. Pure Appl. Chem.*. **1998**, *A35*, 375.
(23) Kwon, Y.; Cao, X.; Faust, R. *Polym. Prepr.* **1998**, *39* (2), 494.
(24) Desponds, O.; Schlosser, M. *J. Organomet. Chem.* **1991**, *409*, 93.
(25) Villesange, M.; Sauvet, G.; Vairon, J. P.; Sigwalt, P. *J. Macromol. Sci.*−*Chem.* **1977**, *A11* (2), 391.
(26) Sigwalt, P. *Macromol. Symp.* **1998**, *132*, 127.
(27) Tsunogae, Y.; Kennedy, J. P. *J. Polym. Sci., Polym. Chem. Ed.* **1994**, *32*, 403.

MA990333K